Australian Meteorological and Oceanographic Journal 62 (2012) 227–245

Temperature variations of southeastern Australia, 1860–2011

Linden Ashcroft, David Karoly and Joëlle Gergis
School of Earth Sciences, University of Melbourne

(Manuscript received April 2012; revised November 2012)

This study presents the first quality-controlled dataset of surface air temperature observations for 1860–1909 across southeastern Australia. Long-term monthly maximum and minimum temperature records from 38 stations in Victoria, South Australia, New South Wales and southern Queensland were identified from the Australian Bureau of Meteorology observational network to provide continuous data coverage from 1860–1950. Detailed homogenisation was undertaken using metadata collected from station history files and a two-step statistical process that involved individual station adjustments and comparison with neighbouring reference series.

The homogenisation process removed many non-climatic changepoints in the previously unexamined 1860–1909 period. Importantly, the impact of the systematic change to Stevenson thermometer screens at the beginning of the 20th century appears to have been minimised. The homogenisation process also reduced the variability of pre-1910 data across the station network, making it comparable with that of the current high-quality temperature record. The adjusted dataset showed very high correlations with the newly developed high-quality observational dataset currently used in Australian climate research (ACORN–SAT) for the overlapping 1910–1950 period.

Combining the 1860–1950 data with ACORN–SAT data for southeastern Australia enabled temperature variations for 1860–2011 to be studied for the first time. A cooling of maximum and minimum temperatures was identified over 1872–1875 and 1891–1894, as well as high interannual variation in temperature from 1885–1890. The link between El Niño–Southern Oscillation (ENSO) and southeastern Australian temperature was found to have fluctuated over 1860–2011, with periods of weak correlations identified in the 1890–1900s, 1920–1930s and the 1960–1970s. These fluctuations were not found to be associated with any particular phase of the Interdecadal Pacific Oscillation, previously reported to modulate the influence of ENSO on the Australian climate.

Trend analysis confirmed that the 1.1 °C increase in maximum temperature and 0.9 °C increase in minimum temperature since 1960 are the largest and most significant trends in southeastern Australian temperature in the last 152 years. The new historical temperature dataset for southeastern Australia provides an additional 49 years of important temperature information for Australia's most highly populated region.

Introduction

Southeastern Australia (SEA) is home to over half of Australia's population (Australian Bureau of Statistics 2011) and produces almost a third of the nation's food supply (Murray-Darling Basin Authority 2011). SEA has experienced a warming trend of around 1 °C in maximum temperature and 0.9 °C in minimum temperature since 1950 (Murphy and Timbal 2008; Australian Bureau of Meteorology 2012a) which has been attributed to anthropogenic climate change (Karoly and Braganza 2005). The combination of interannual temperature variability and a large-scale warming trend presents an increased risk of high temperatures, leading to more heat-related deaths in the elderly and disadvantaged (Trenberth et al. 2007; Hasson et al. 2009; Pezza et al. 2011), and a higher likelihood of bushfires (Hasson et al. 2009). It is crucial therefore to study the natural variability of

Corresponding author address: Linden Ashcroft, School of Earth Sciences, University of Melbourne, Victoria, Australia. Ph: +61 38344 7672
Email: l.ashcroft@student.unimelb.edu.au

temperature across SEA as well as the large-scale positive trends that are currently being recorded.

SEA is subject to a highly variable climate, particularly with respect to rainfall (Nicholls et al. 1996a; Murphy and Timbal 2008; Risbey et al. 2009a). This is primarily due to large-scale atmosphere and ocean circulation features such as El Niño–Southern Oscillation (ENSO) (Nicholls et al. 1996a; Murphy and Timbal 2008; Risbey et al. 2009b) and Indian Ocean sea surface temperature fluctuations (Cai et al. 2011). Previous studies have examined the interannual rainfall variability in SEA and how it responds to ENSO and Indian Ocean sea surface temperature changes, best represented by the Indian Ocean Dipole (Murphy and Timbal 2008; Risbey et al. 2009b; Verdon-Kidd and Kiem 2009; Cai et al. 2011; Ummenhofer et al. 2011).

Fewer studies have explored changes in the complex relationship between temperature variability and these large-scale circulation features, although they are known to interact (Lough 1997; Power et al. 1998; Jones 1999; Power et al. 1999a; Jones and Trewin 2000). Power et al. (1998) and Jones and Trewin (2000) identified a strong negative correlation between Australian maximum temperature (Tmax) and ENSO both annually and seasonally: for example, an El Niño event was generally associated with positive Tmax anomalies and a La Niña event with negative Tmax anomalies. The minimum temperature (Tmin)–ENSO relationship was found to be more complex. El Niño events led to below-average Tmin in the winter, due to a greater amount of nocturnal cooling because of decreased cloud cover. In the summer however, El Niño events were linked to above-average Tmin as a result of the influence of above-average Tmax values on Tmin, as well as the rate of nocturnal cooling (Power et al. 1998; Jones 1999; Jones and Trewin 2000).

High temperature–ENSO correlations are primarily due to the influence of rainfall on temperature. SEA rainfall is highly influenced by ENSO, and temperature in turn is influenced by rainfall and associated cloud cover (Jones 1991; Nicholls et al. 1996a; Power et al. 1998; Jones 1999; Power et al. 1999b; Alexander et al. 2007). Power et al. (1998; 1999b) explained that this could be understood physically: a period of high rainfall (with an associated increase in soil moisture) and increased cloud cover reduces the short-wave radiation and increases the latent heat flux between the ground and the atmosphere. This manifests as an out-of-phase relationship between rainfall and maximum temperature (Tmax) and an in-phase relationship between rainfall and minimum temperature (Tmin). The rainfall–temperature relationship was found to be dominant across Australia, although weaker along the coast and at exposed sites (Power et al. 1998).

The relationship between Australian climate and ENSO has not remained stable over time. Weak correlations between ENSO and Australian rainfall have previously been identified in the 1920–1950 period (Lough 1997; Reason et al. 1998; Kestin et al. 1998) and the first half of the 19th century (Gergis et al. 2012a). One modulating factor in the ENSO–SEA climate relationship is the Inter-decadal Pacific Oscillation (IPO), first described by Power et al. (1999a) as a Pacific basin-wide index of the North Pacific Decadal Oscillation (Folland et al. 1997, 2002; Mantua et al. 1997). ENSO events are known to have a strong influence on eastern Australia rainfall during negative phases of the IPO (Power et al. 1999a; Kiem et al. 2003), when convection over the equatorial Western Pacific becomes greater and moves closer to the eastern Australian coast (Cai and van Rensch 2012).

Power et al. (1999a) also found that ENSO was highly correlated with Australian-wide temperature and rainfall from 1910–1997 when the IPO was in a negative phase, but not when the IPO was positive. As rainfall–temperature variations are closely linked (Power et al. 1998; Trenberth and Shea 2005) these results suggest there may also be a low-frequency variation in the influence of ENSO on SEA temperature. However, the current temperature and rainfall datasets available for SEA begin in 1910 and 1900 respectively (Torok and Nicholls 1996; Lavery et al. 1997; Della-Marta et al. 2004; Trewin 2012), restricting the ability to examine decadal fluctuations in the ENSO–SEA climate relationship (Nicholls et al. 1996b; Power et al. 1999a; Murphy and Timbal 2008).

Pre-1900 rainfall variation in SEA have been examined in several studies (Ummenhofer et al. 2009; Verdon-Kidd and Kiem 2009; Timbal and Fawcett 2012), but pre-1910 temperature fluctuations have not been explored due to issues with observation standards (Trewin 2010). Before 1908, Australian station coverage was not as dense as today's temperature network, and there was no standard procedure for recording temperature across the country (Parker 1994; Nicholls et al. 1996c; Torok 1996). At the start of the 20th century the Australian Bureau of Meteorology (the Bureau) was formed and there was a systematic conversion to standard observing practices, including a change from Glaisher temperature screens to Stevenson screens (Nicholls et al. 1996c). The uncertain quality of the pre-1910 data and the lack of readily available metadata means that the current high-quality temperature dataset available for Australia does not begin until 1910 (Della-Marta et al. 2004; Trewin 2012). However, this does not mean that valuable observations were not taken in the 19th century, or that the spatial coverage of these observations is too poor to be useful in regional studies.

The period from 1860 to 1910 was one of rapid growth in Australian meteorology, led by a small group of passionate men dedicated to the rigorous observation of the nation's weather and climate (Gentilli 1967; Moyal 1986; Day 2007; Douglas 2007). Colonial government observatories were built in the 1850s in Sydney and Melbourne, where official meteorological observations began for those cities and continue to the present day. The Government Astronomers and Meteorologists of the colonies—William Scott and Henry Chamberlain Russell of New South Wales, Robert Ellery and Georg Neumayer in Victoria, Charles Todd from South Australia and Clement Wragge in Queensland—not only maintained local weather records but also developed observational networks across their colonies (Day 2007).

Many of the stations set up by these meteorological pioneers are still open, and provide the basis for the pre-20th century temperature observation network used in this study. These historical data are an untapped resource that, if processed appropriately, could provide valuable information on natural temperature variability to further the study of past, present and future climate (Nicholls et al. 2006).

The aim of this paper is to extend the SEA temperature record by improving the quality of observational Tmax and Tmin data in the region from 1860–1909. This will significantly extend our knowledge of 19th century climate in SEA, and place modern temperature variations and the influence of large-scale circulation patterns in a longer-term context. After outlining the data used in the study, we describe the detailed two-step homogenisation process employed to minimise inhomogeneities in the pre-1910 temperature data. The two-stage process combines individual station analysis and metadata with statistical techniques that identify discontinuities in a time series and significant changes in the difference between data from a station of interest and data from a reference series. This approach aims to overcome the difficulties of homogenising historical temperature data, including low spatial density and large error values (e.g. Brunetti et al. 2006).

The quality of the homogenised dataset is then tested by comparing it to high-quality observational and gridded data products for SEA. We examine temperature variability in the previously unexamined 1860–1909 period, and look at the relationship between SEA temperature and ENSO over the last 150 years. Finally we conduct preliminary trend analysis on the 1860–2011 temperature data for SEA to determine the significance of the positive temperature trends seen in the region since 1960 (Murphy and Timbal 2008; Fawcett et al. 2012).

Data

Long-term temperature station selection

The process of data preparation, quality control and homogenisation is outlined in Fig. 1 and described in the following two sections. The stations with long-term temperature data that were used in this study are shown in Fig. 2. The temperature stations used in this study were selected based on the following three criteria:

1. *Located within SEA (138°–154°E, 24°–40°S)*
   SEA was defined as the Bureau rainfall districts 19–26 and 40–90 within Victoria, New South Wales, eastern South Australia and southern Queensland in the domain 138°–154°E, 24°–40°S (Australian Bureau of Meteorology 2010).
2. *Digitised monthly temperature records available before 1890*
   This period was chosen to ensure that at least 20 years of additional temperature information could be analysed. Stations with less than one year of observations in the pre-1890 period were excluded. Many of the excluded

Fig. 1. An outline of the data collection and homogenisation process used in the development of the SEA38 for 1860–1950.

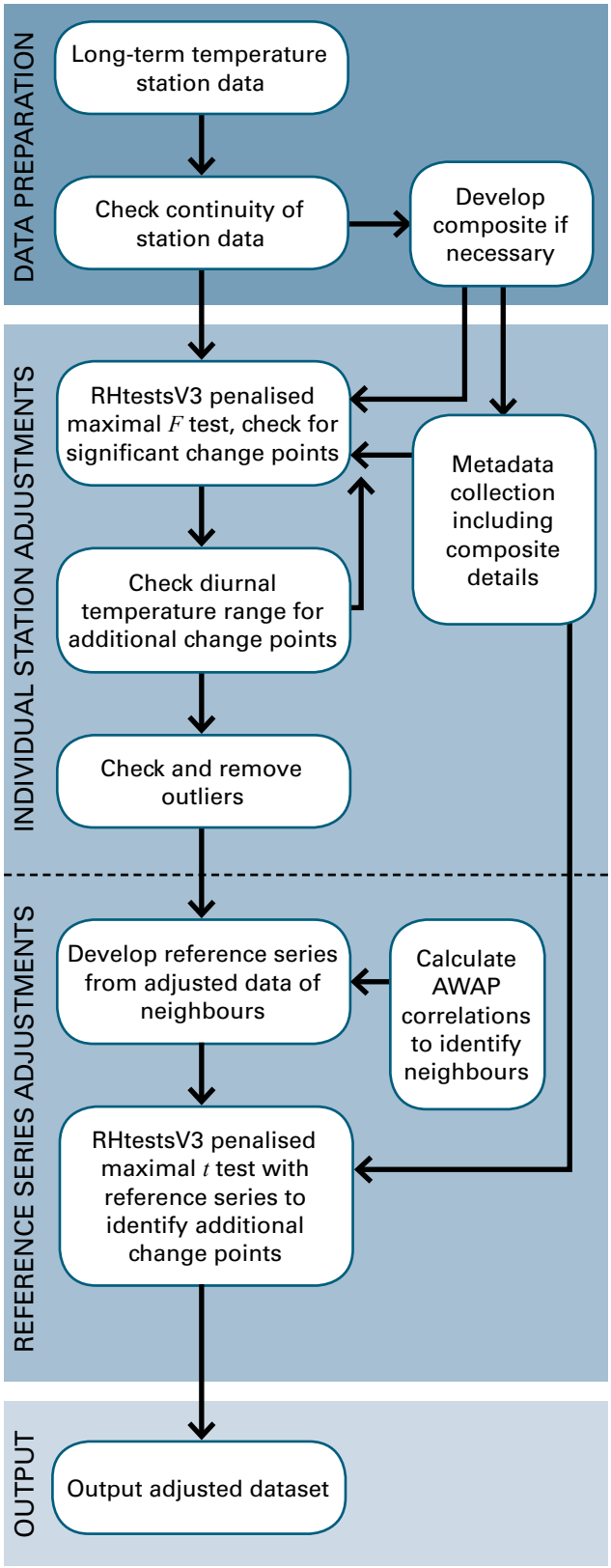

Fig. 2. Long-term temperature stations in SEA with data from 1860. The stations are marked according to the period in which observations began: before 1860 (asterisk), between 1860 and 1869 (diamond), between 1870 and 1879 (triangle) and between 1880 and 1890 (square).

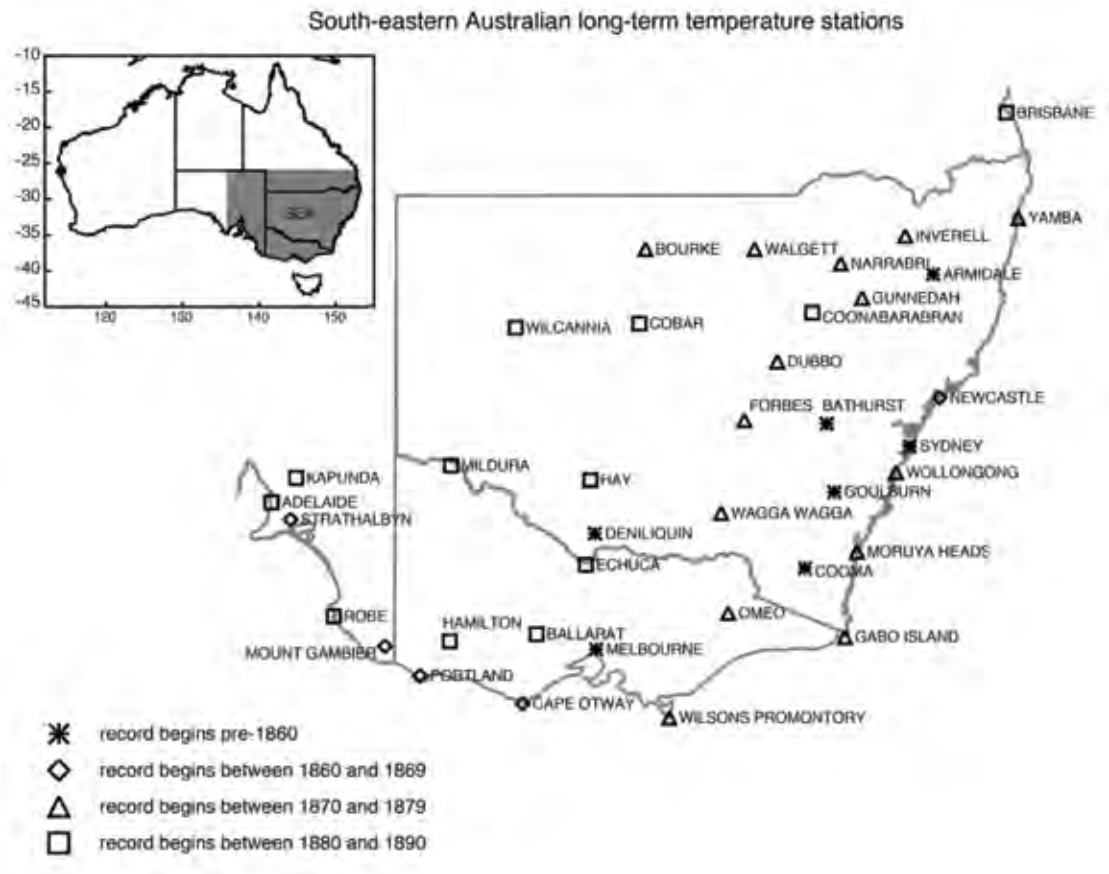

stations came from Queensland, as Clement Wragge only took up his position in 1887 and opened stations during 1887–1890 (Day 2007).

3. *Temperature record continuing to the end of 2009*
   Having data to the present day would allow for a comparison with the current high-quality temperature data for SEA. The present day was taken as the end of 2009. If a single station did not meet this criterion, then a composite series was developed using neighbouring stations.

A total of 38 temperature stations satisfied all three criteria (see Fig. 2 and Table 1). This network will henceforth be referred to as SEA38. Monthly Tmax and Tmin values were obtained from the Bureau's digital Australian Data Archive for Meteorology (ADAM) database (Australian Bureau of Meteorology 2000). Pre-1972 observations were converted from degrees Fahrenheit to degrees Celsius (Trewin 2012) by the Bureau. While modern temperature observations in the ADAM database undergo detailed quality control, pre-1910 records have only received rudimentary quality analysis or have not been assessed for quality before digitisation (K.Rowney, personal communication).

Stations from the newly developed Australian Climate Observational Reference Network – Surface Air Temperature (ACORN–SAT) temperature dataset (Fawcett et al. 2012; Trewin 2012) were used to provide high-quality annual and seasonal Tmax and Tmin data for SEA from 1910–2011. The 49 ACORN–SAT stations in the SEA region were used to represent SEA: this network will henceforth be known as ACORN–SAT49. A total of 23 stations are common to both SEA38 and ACORN–SAT49. These common stations are marked with an asterisk in Table 1. Analysis was also conducted using the previous annual high-quality temperature datasets developed by Torok and Nicholls (1996) and updated by Della-Marta et al. (2004), with very similar results. Additional monthly Tmax and Tmin data from the Australian Water Availability Project (AWAP) 0.05°x 0.05° temperature grid (Jones et al. 2009) were used to develop station reference series. Data from the gridpoints closest to each station in SEA38 were used, and will be referred to as the AWAP38 gridpoint network. Area-averages of the gridpoint and station data used in later analysis were calculated using Thiessen polygons (Thiessen 1911).

Monthly Southern Oscillation Index (SOI) values—the mean pressure difference between Tahiti and Darwin—were obtained from the Bureau for 1876–2011 (Australian Bureau of Meteorology 2011) to represent variations in ENSO. The Niño 3.4 sea surface temperature index was derived for 1876–

Table 1. Details of composite temperature stations in the 38-station temperature network (SEA38) used in this study. Composite stations developed using an adjusting technique are labelled AC, while those developed using a simple composite technique are labelled SC (see data section for details). If the Tmin composite details differ to Tmax, they are shown in brackets. AWAP indicates that temperature data from the nearest 0.05° x 0.05° Australian Water Availability Project (Jones et al. 2009) gridpoint were used. Asterisks indicate stations that are also part of the high-quality ACORN–SAT network (Trewin 2012).

Location	*Station*	*Period*	*Months of overlap and composite type*			
Adelaide*	23000	2/1887–3/1955	288	AC		
	23034	4/1955–12/2009				
Kapunda*	23307	1/1885–10/1952	30	SC		
	23321	11/1952–9/1996			142	AC
	23373	10/1996–12/2009				
Strathalbyn	23747	1/1861–1/1900	1111 (1108)	AC		
	23703	2/1900–1/1925			543 (531)	AC
	23747	2/1925–8/1996	57 (55)	SC		
	24580	9/1996–12/2009				
Mount Gambier*	26020	1/1861–2/1942	120	AC		
	26021	3/1942–12/2009				
Robe*	26026	9/1884–12/2009				
Brisbane*	40214	1/1887 to 3/1994	0	SC		
	40842	4/1994 to 12/2009				
Wilcannia*	46043	1/1881–12/2009				
	(AWAP)	(1/1940–1/1957)	967	AC		
Cobar*	48030	3/1881–5/1962	31	SC		
	48027	6/1962–12/2009				
Bourke*	48013	5 (8)/1871–11/1994	1	SC		
	48239	12/1994–12/1998			13	SC
	48245	1/1999–12/2009				
Walgett*	52026	8/1878–5/1993	0	SC		
	52088	6/1993–12/2009				
Narrabri	54120	1(11)/1871–1/1962	0	SC		
	53030	1/1962–7/2001			12	SC
	54038	8/2001–12/2009				
Gunnedah	55023	12/1876–12/2009				
Armidale	56002	12/1857–12/1930	749 (737)	AC		
	56016	1/1931–12/1956			258 (269)	AC
	56002	1/1957–5/1997	0	SC		
	53037	7/1997–12/2009				
Inverell*	56017	3/1874–3/1995	33 (23)	SC		
	56242	4/1995–12/2009				
Yamba*	58012	6/1877–12/2009				
Newcastle	61055	1/1862–12/2009				
Bathurst*	63004	1(2)/1858–1/1909	694 (735)	AC		
	63005	2/1909–12/2009				
Coonabarabran	64008	4/1879–12/2009				
Dubbo*	65012	1/1871(3/1872)–2/1993	82 (71)	AC		
	65070	3/1993–12/2009				
Forbes	65016	1(4)/1873–1/1996	4 (0)	SC		
	65103	2/1996–12/2009				

Location	*Station*	*Period*	*Months of overlap and composite type*			
Sydney*	66062	1/1859–12/2009				
Wollongong	68069	1/1871–5/1950	2 (0)	SC		
	68053	6/1950–11/1970			62	AC
	68188	12/1970–5/1997	131 (122)	AC		
	68228	6/1997–12/2009				
Moruya Heads*	69018	1/1876–12/2009				
Goulburn	70037	1/1858–6/1967	0	SC		
	70210	7/1967–9/1971			0	SC
	70263	10/1971–1/1975	0	SC		
	70285	2/1975–6/1978			0	SC
	70263	7/1978–12/2009				
Cooma	70023	1(2)/1858–1/1957(12/1956)	6 (0)	SC		
	70094	2/1957 (1/1957)–1/1971			0	SC
	70278	2/1971–12/2009				
Wagga Wagga*	72151	11(5)/1871–2/1942 (1/1943)	107 (96)	AC		
	72150	3/1942 (2/1943)–12/2009				
Deniliquin*	74128	3/1858(3/1867)–7/1997(1/1998)				
	74258	8/1997(2/1998)–12/2009	67(60)	AC		
Hay	75031	1/1881–12/2009				
Mildura*	76077	7/1889–8/1946 (6/1946)	54 (22)	SC		
	76031	9/1946 (7/1946)–12/2009				
Echuca	80015	6/1881–12/2009				
Omeo	83025	1(4)/1879–12/2009				
Gabo Island*	84016	2/1877–12/2009				
Wilsons Promontory*	85096	3/1877–12/2009				
Melbourne*	86071	5/1855–12/2009				
Ballarat	88015	7/1879–12/1907	580 (581)	AC		
	89002	1/1908–12/2009				
Cape Otway*	90015	4/1864–12/2009				
Portland	90070	1/1863–1/1957	0	SC		
	90014	2/1957–6/1982			176	AC
	90171	7/1982–12/2009				
Hamilton	90044	1/1886–7/1983	0	SC		
	90173	8/1983–12/2009				

2011 as a secondary ENSO index from the Hadley Centre Global Sea Ice and Sea Surface Temperature and National Centers for Environmental Prediction datasets (Reynolds and Smith 1994; Rayner et al. 2003, www.cgd.ucar.edu/cas/catalog/climind/TNI_N34/index.html). The Niño 3.4 index is the five-month smoothed normalised anomalies from the area-averaged sea surface temperatures over 170°W–120°W, 5°S–5°N (Trenberth 1997; Trenberth and Stepaniak 2001).

Seasonal IPO values for 1850–2009 smoothed using a 13-year Chebyshev filter were obtained from the UK Met Office Hadley Centre for Climate Change (Folland 2008). The IPO is defined as the third leading empirical orthogonal function of 13-year low-pass filtered global sea surface temperatures (Power et al. 1999a). Negative IPO phases manifest as cool temperature anomalies in the tropical Pacific, similar to La Niña sea surface temperature (SST) pattern, while the positive phase is associated with above-average tropical Pacific SSTs, or El Niño–like conditions (Power et al. 2006). IPO data before 1875 were regarded as potentially unreliable (Folland 2008), so only 1876–2009 data were considered.

Composite series development

For many of the locations shown in Fig. 2, it was necessary to merge two or more station records to develop a continuous temperature series to the end of 2009. These are known as composite stations. It is recommended that stations have an overlap of at least five years of monthly data (with a minimum

of two years) before they can be combined into a single series (World Meteorological Organization 2003; Trewin 2010). This allows the relationship between the two stations to be assessed for their use in extending the temperature record. While an overlap of this length is ideal, nearby stations that do not meet this criterion can still be combined and are treated as a single station series with a known inhomogeneity at the time of station change (Street et al. 2007).

Composite stations were identified by their distance from the station of interest and their ability to fill the data gap in the original station record. The majority of composite stations were less than 20 km apart and were similar to those used in the development of the ACORN–SAT and previous high-quality temperature datasets (Torok 1996; Trewin 2012). If there were no appropriate neighbouring stations, and more than ten consecutive years of data were missing, monthly temperature data from the closest gridpoint in the AWAP38 gridpoint network were used. This was only required for the minimum temperatures of Wilcannia (046043) for 1940–1957. Depending on the amount of data overlap between each station, the composite series were then developed using the following two methods:

1. *Simple composite*
   If there were less than five years of data overlap (i.e. 60 monthly records) then the two series were merged with no adjustment. The observations from the newer station were used as soon as they became available and the values from the older station during the overlap period were discarded.
2. *Adjusted composite*
   If there were more than five years of overlapping data, the older series was adjusted relative to the newer station records using a simple constant–difference technique. The monthly averages of the newer station during the overlap period were calculated and added to the anomalies of the older station (relative to the older station average for the overlap period). These adjustments have the effect of making records from the older station consistent with that of the newer station.

If a composite was made up of more than two stations, the process was applied to each overlapping period iteratively, beginning with the most recent observations. The month and year of each station change was recorded and added to the station metadata as a possible changepoint. Details of the composite technique and stations used for each location are given in Table 1, and Fig. 3 shows the final number of stations with data for each year from 1850 to 1950. The year 1860 was chosen as the start year for analysis as there were only seven stations with data before this date.

Metadata sources

Details of pre-1900 New South Wales, Queensland and South Australian stations were located in hand-written instrument books housed in the rare book room of the Bureau's National Meteorological Library in Melbourne (manuscript numbers MS17–19, 22 and 28). The books contain details of instrument

Fig. 3. Number of stations in SEA38 with maximum temperature (Tmax, solid line) and minimum temperature (Tmin, dashed line) data each year from 1850–1950.

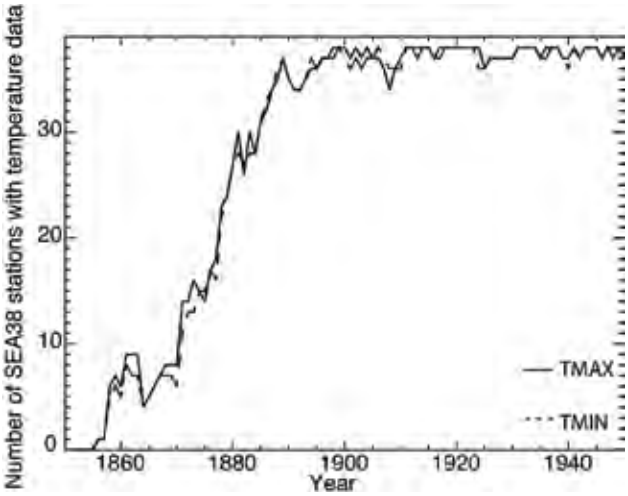

replacements, changes in observer, the dates of thermometer screen changes and occasionally site moves. Similar books for Victorian stations were found in the Victorian branch of the National Archives of Australia (NAA series numbers B5310–B5312).

Metadata collection for modern weather stations at the Bureau is done through the digital repository 'SitesDB', but this source does not contain detailed information on changes that occurred before about 2000 (Australian Bureau of Meteorology 2012b). For earlier metadata, it was necessary to gather information from the paper station history files kept at the Bureau's Head Office in Melbourne. The station history files contain detailed correspondence on instrument changes, site moves, screen replacements and other station idiosyncrasies. These files provide a good idea of the quality and history of many of the oldest weather stations in Australia. Additional metadata were also gathered from network station history summaries developed by Torok (1996).

Temperature data homogenisation method

Temperature measurements are very sensitive to changes in observing conditions and practices, making them susceptible to artificial trends and discontinuities (Parker 1994; Trewin 2010). It is important to identify and remove as many of these inhomogeneities as possible, to ensure that only true changes in the temperature observations remain (Conrad and Pollak 1950). This is especially the case for early instrumental measurements that have been observed in a way which does not conform to modern national and international observing guidelines (Australian Bureau of Meteorology 1997; World Meteorological Organization 2008; Trewin 2010). There are many statistical techniques that have been developed to identify and adjust for inhomogeneities (Peterson et al. 1998; Ducrè-Robitaille et al. 2003; DeGaetano 2006; Reeves et al. 2007; Venema et al. 2012). The standard normal homogeneity test (SNHT) (Alexandersson 1986;

Menne and Williams 2009) has previously been identified as a preferred homogenisation technique to use if there is a reliable reference series available with which to compare the data from the station of interest (Ducrè-Robitaille et al. 2003; DeGaetano 2006; Reeves et al. 2007). This approach examines the normalised difference between the station of interest (hereafter known as the candidate station) and a reference series. A discontinuity is identified when there is a significant change in the difference between the two stations. However, this process requires a reliable reference series, or a large network of neighbouring stations, both of which are often difficult to obtain when using early temperature records. Additionally, a reference series approach is unable to detect a network-wide change on observing practice, such as the Australia-wide conversion to Stevenson screens at the start of the 20th century (Slonosky and Graham 2005)

Regression-based techniques such as the two-phase regression (TPR) or multi-phase regression procedures (Easterling and Peterson 1995; Vincent 1998; Lund and Reeves 2002) have been found best for identifying discontinuities in data with a constant trend, without the use of a reference series (Ducrè-Robitaille et al. 2003; Reeves et al. 2007). These procedures calculate a linear regression on either side of a point, and determine the residual sum of squares for each regression: the point that provides a minimum for this sum is the most likely changepoint (Easterling and Peterson 1995).

Regardless of the statistical technique used, all research into identifying inhomogeneities values the use and maintenance of detailed metadata (Peterson et al. 1998; Aguilar et al. 2003). Metadata provide information about the observation site and, importantly, document changes made to instrumentation, site exposure and station location. These data make it easier to identify and attribute discontinuities in the climate record, rather than relying on statistical analysis alone (Rhoades and Salinger 1993; Wang et al. 2007).

RHtestsV3

The RHtestsV3 software package has been developed by the Expert Team on Climate Change Detection and Indices (Wang et al. 2007; Wang 2008a; ETCCDI 2009; Wang and Feng 2010). The RHtestsV3 package combines extensions of the SNHT and TPR to allow for the identification of changepoints with or without a reference series, and is able to adjust the timing of statistically identified changepoints to take metadata into account. The package also includes empirically developed penalty functions, known as the penalised maximal F and t tests, relating the changepoint significance to the location of the changepoint within the time series (Wang et al. 2007; Wang 2008a). This accounts for the tendency of both the SNHT and TPR to overestimate the number of changepoints at the start and end of a series and, in the case of the TPR, also in the middle of a series (Wang et al. 2007; Wang 2008a).

The RHtestsV3 package identifies changepoints that are significant without metadata support (with respect to a user-defined level of significance) and changepoints that are only significant if they are supported by documented changes (Wang and Feng 2010). The dates of these changepoints can be manually altered to reflect metadata. The RHtestsV3 package can be applied to annual, monthly, or daily data, and has been used successfully for a wide range of variables (e.g. Wang 2008b; Alexander et al. 2010; Wang et al. 2010; Cornes et al. 2012).

In this study, we use both components of the RHtestsV3 to conduct an innovative two-step homogenisation procedure. In step one, data are examined from individual stations, using metadata and the penalised maximal F test to adjust for inhomogeneities. Step two uses these adjusted records to build reference series for each station, allowing additional relative inhomogeneities to be identified using the penalised maximal t test. This process study is similar to methods employed in the development of other regional historical climate series, in that it follows an iterative procedure of identifying and adjusting discontinuities using station history information and statistical techniques (Easterling et al. 1996; Vincent and Gullett 1999; Barring et al. 1999; Brunetti et al. 2006; Alexander et al. 2010; Jones et al. 2012; Trewin 2012). However, examining and adjusting the data of each station individually before identifying relative inhomogeneities with reference series is a new approach that aims to overcome the low station density and large errors present in the early temperature records of SEA and many historical station networks.

Step 1: Individual temperature station adjustment

In the first round of data homogenisation (Fig. 1), the penalised maximal F test from the RHtestsV3 package was applied to the finalised monthly data from each station in SEA38. The test was applied to an early subseries of the data (Period 1, 1860–1950), a later subseries (Period 2, 1910–2009) and the whole series (Period 3, 1860–2009). This was done to minimise the influence of recent warming trends on the earlier parts of the series, as the maximal F test assumes a constant trend (Wang 2008a). Running the tests on the shorter subperiods increases the uncertainty of the results (X.Wang, personal communication), so changepoints were compared across each of the periods to check their validity. If a documented changepoint was identified in Period 3 but not in Period 1, for example, it was added to the Period 1 changepoints and retested to determine if the change was significant in the subseries.

The program was run once on each subseries for each station to identify changepoints that were statistically significant without supporting metadata and changepoints that were only significant if there was accompanying station history information. All changepoints were then assessed against the station history files using a 95 per cent statistical significance level. If a changepoint was identified within six months of a noted station event (e.g. a thermometer change, composite station change or site move), the date of the changepoint was updated and retested. The diagnostic graphics output with each run of the program were also examined to assess the magnitude of the changepoints and

whether they made physical sense. For example, a change from a non-standard Glaisher screen to a Stevenson screen would be expected to produce a decrease in the maximum temperatures, as Glaisher screens offer inadequate protection from solar radiation and have been associated with an overestimation of Tmax (Nicholls et al. 1996c; Trewin 2010).

Changepoints that were not significant were deleted, and the process repeated again until all changepoints became statistically significant, or were assigned significance due to supporting metadata information. The diurnal temperature range (DTR) of the original series for each station in SEA38 over Period 1 was also checked to search for additional changepoints that may be supported by metadata. Each changepoint identified in the DTR series was cross-referenced against changes found in the Tmax and Tmin series. If the changepoint had not been picked up already in either temperature series, then the date was added to the list of changepoints for both, and retested for significance.

Unfortunately, the adjustments over Periods 2 and 3 (1910–2009, 1860–2009) introduced large false positive trends in the data of many stations. This is due to the substantial increase in observed temperatures since 1950 (CSIRO and the Australian Bureau of Meteorology 2012) and the fact that the F test assumes a constant trend when identifying inhomogeneities (Wang 2008a). The positive trends that were forced across the entire time series led to unrealistically low values for the pre-1910 data of many stations, and made it impossible to create a continuous adjusted time series from 1860–2009. Because of these induced trends, it was decided that the focus be moved to the Period 1 results only. Future improvements to the RHtests will include the ability to account for a trend change (Wen et al. 2011).

In Period 1, 141 (161) changepoints were identified for Tmax (Tmin), 58 (52) per cent of which were supported by metadata. This is approximately the same percentage of changepoints supported by metadata in the ACORN–SAT dataset (Trewin 2012). It was encouraging to see that many of the 19th century changepoints could be explained by changes in instruments or screens. For example, the systematic change of thermometer screens in rural South Australia in 1892 was individually identified in the Tmax record for all four affected South Australian stations. In fact, changes from a Glaisher stand (or other type of thermometer screen) to a Stevenson screen in the early 20th century were identified in 18 (9) of the 38 Tmax (Tmin) station records, with an additional six (five) changepoints also attributed to earlier changes in the type of thermometer screen e.g. the change from a Glaisher stand to a large shed in Sydney in 1869. There were only five stations where the change to a Stevenson screen was recorded in the metadata but not identified as a significant changepoint in the Tmax or Tmin time series. Changepoints that were unsupported by metadata were often clearly identifiable from a visual inspection of the data. In general, composite station changes were not identified as significant changepoints.

The first round of individual station adjustments identified by the RHtestsV3 package were applied to SEA38 network for Period 1. The outlying values of the adjusted monthly anomalies (defined as values ±3 standard deviations from the mean anomaly over Period 1) were then examined individually to check for erroneous values. If a particular month was tagged as an outlying value by three or more stations it was manually examined for spatial coherence, and often retained as a plausible event i.e. it was an exceptionally cold or warm month, rather than an erroneous value. This step was applied to the adjusted data, rather than the original data, because many of the unadjusted data in the pre-1900 period were unrealistically high or low due to the differences between the early observing practices and the standard procedure used today. These data would have been identified as outlying values in their unadjusted state and deleted, removing potentially important data for this study.

Step 2: Reference series adjustments

After adjusting individual station data on the basis of metadata and the penalised maximal F-test, we then developed reference series for each station in SEA38. Recent research into homogenisation techniques suggests that relative homogeneity testing is preferable to individual station testing, because examining station data relative to neighbouring stations minimises the likelihood of real climatic changes being falsely identified as inhomogeneities (Peterson et al. 1998; Venema et al. 2012). However, due to the non-standard observing practices of pre-1910 SEA temperature records compared to modern observation procedures, we concluded that little useful information could be obtained from a reference series comprising of pre-1910 station data if they had not undergone some individual homogenisation testing first.

The stations used for each reference series were identified using the relationship between the data from AWAP38, the network of AWAP gridpoints closest to each station in SEA38. Correlations were calculated between the monthly Tmax and Tmin anomalies (compared to the 1961–1990 climatology) at each of the 38 gridpoints. An example of this is shown for Sydney in Fig. 4. The correlations between the gridpoint closest to Sydney and all AWAP gridpoints are plotted, with the locations of the other AWAP38 network members also marked. For the majority of gridpoints in AWAP38, at least six of the gridpoints representing neighbouring SEA38 stations were highly correlated (Pearson correlation coefficient $r >$ 0.85). Only the coastal gridpoints, (e.g. Gabo Island, Wilson's Promontory and Yamba) had fewer highly correlated SEA38 neighbours; generally two or three.

Correlations between the AWAP38 network gridpoints represent how monthly temperature anomalies at each station in SEA38 should theoretically relate to each other. In reality, the observations (particularly in the early period) are not as well correlated due to remaining data inhomogeneities. Correlations between the monthly anomalies (relative to the 1910–1950 period) of the adjusted Period 1 SEA38 data

Fig. 4. Correlations between AWAP monthly anomalies (relative to the 1961–1990 base period) at the gridpoint closest to Sydney, and the AWAP 0.05° x 0.05° gridded temperature anomaly data for (a) Tmax and (b) Tmin, 1900–2009. Locations of gridpoints in the AWAP38 gridpoint network are marked with a thick black asterisk or white square. Stations marked with a white square (Wollongong, Moruya Heads, Goulburn, Bathurst, Armidale and Newcastle) were used in the development of a Sydney reference series.

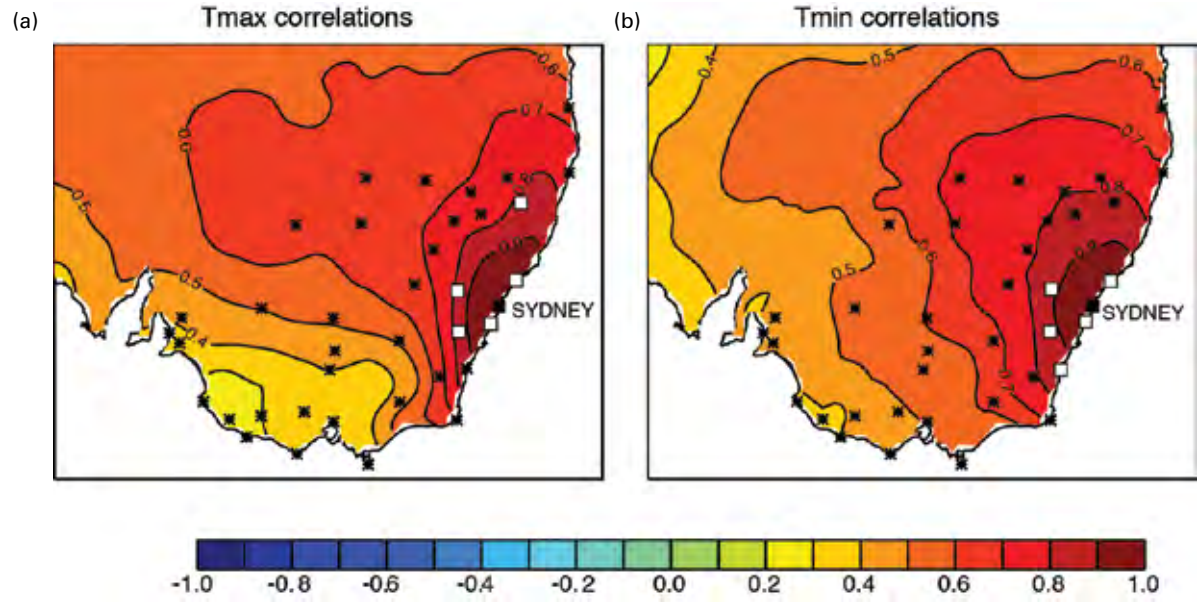

were calculated and compared to the AWAP38 gridpoint correlations. The correlations between SEA38 stations were lower than that of the equivalent AWAP38 gridpoints by a Pearson's correlation coefficient (r) value of 0.1 or more. In some cases, particularly for coastal stations, the correlations were much lower for the observational data than for the AWAP38 gridded data. In general though, the stations that were highly correlated using the AWAP38 monthly gridpoint data were also highly correlated using SEA38 monthly station data.

A station was used in the reference series of a candidate station if the two stations were highly correlated using the AWAP38 network data ($r > 0.7$) and the adjusted Period 1 SEA38 station data ($r > 0.5$). A minimum of three and maximum of five stations were used in the development of each reference series, to reduce the impact of potential inhomogeneities remaining at the neighbouring stations and to ensure that the neighbouring stations were confined to the local region surrounding the candidate station (Peterson and Easterling 1994). The neighbouring stations used in the development of Sydney's reference series are marked in Fig. 4 as an example. A number of stations did not have enough highly correlated neighbours for a reference series to be built. They are listed in Table 2, and are coastal stations, or inland stations in data sparse regions. Table 2 shows that more stations failed to have reference series for Tmin than for Tmax. This could reflect the greater influence that small-scale factors have on near-surface conditions at night (Jones and Trewin 2000).

Reference Series (RS) development is shown mathematically for a station of interest s in Eqn. 1. Each reference series was built using the sum of monthly anomalies weighted by the square of the observational correlation between the candidate station and the neighbouring stations. The sum of weighted anomalies was added to the final year of data (1950 monthly values) for the candidate station. If the year 1950 contained any missing values then data from 1949 were used, as the mean of the reference series should not affect the adjustment procedure (Peterson and Easterling 1994).

$$RS_{s,1} = T_{s,0} + \left(\sum_{k=1}^{n} \rho_k^2 T'_{k,1}\right) \times \left(\sum_{k=1}^{n} \rho_k^2\right)^{-1} \quad ...(1)$$

where:

$T_{s,0}$ = monthly temperature at the candidate station for the most recent full year of observation

ρ = Pearson correlation coefficient of neighbour station (minimum=0.5)

T' = monthly temperature anomalies of neighbour station compared to 1910–1950

n = number of correlated neighbour stations (minimum=3, maximum=5).

The penalised maximal t test (Wang et al. 2007) was then used to compare the candidate station to its reference series, identifying possible changepoints. As the reference series were not guaranteed to be homogenous, a higher significance value was set on the changepoints (99 per cent) and changepoints that were significant even without metadata support were examined. This additional round of adjustments identified 44 (29) changepoints for Tmax (Tmin). They were smaller in size than those found in the single-

station adjustments and in general were not supported by metadata, possibly because most large changepoints with metadata support were identified in the first round of adjustments.

The final number of adjustments per decade from 1860–1950 is shown in Fig. 5. The distributions are similar for Tmax and Tmin, and show that the majority of adjustments occurred in the three decades from 1880–1909. This is when most stations transitioned to Stevenson screens (Nicholls et al. 1996c). The higher number of Tmax adjustments during 1910–1919 is due to a large number of changepoints identified using reference series, possibly refining some of the adjustments made in the individual station adjustments.

Data quality of the 1860–1950 SEA temperature network

Figure 6 shows the area-averaged annual Tmax, Tmin and DTR anomalies (compared to the 1910–1950 mean) for the original SEA38 data, the adjusted SEA38 data and the ACORN–SAT49 temperature network data from 1860–1950. The annual maximum and minimum anomaly across the stations in each network is also plotted in Fig. 6, to indicate the complete range of temperature variation over 1860–1950. It is important to remember the temporal and spatial coverage of SEA38 when examining these results, particularly for the decade of 1860–1869. Figure 3 shows that there are only 12 stations with data before 1870. This reduced coverage may indicate that the early part of the record is not representative of the wider SEA region and may also explain why the earliest ten years of data display a reduced range of temperature variation (pink shading in Fig. 6), particularly for Tmin. However, the area-averages for 1860–1950 calculated using the 12 stations with data before 1870 alone (not shown) compare very well to the area-average calculated using the whole SEA38 network ($r \geq 0.80$ for Tmax, Tmin and DTR). It is therefore fair to say that the 1860–1869 area-average calculated using a smaller network still provides valuable information about temperature variations across SEA.

There are two clear improvements in the adjusted temperature data over 1860–1909. The first is a decrease in the range of temperature variability across the network. Greater temperature variability can still be seen before 1910 (pink shading in Fig. 6), but it is not nearly as great as in the original values (grey shading in Fig. 6). In fact, the variability in the adjusted network is similar in magnitude to that of the 49 ACORN–SAT stations within SEA (blue broken lines in Fig. 6). Similar results were obtained when examining the 23 stations common to both SEA38 and ACORN–SAT49 (not shown). The reduction of variability across the network is further illustrated in Fig. 7, which shows the standard deviation of the annual temperature anomalies at each station in a moving 30-year window, averaged over all stations, for the original and adjusted values for each station in SEA38. Values from the AWAP38 gridpoint network were combined with the adjusted SEA38 data using the constant–difference method to calculate the standard deviations across SEA38 for 1860–2009. The average standard deviations of the adjusted SEA38 data before 1910 are much more consistent with 1950–2009 values than the standard deviations of the original SEA38 values for Tmax, Tmin and the DTR.

The second improvement is the reduction of a step change at 1908–1910, particularly for Tmax and DTR (step down) but also for Tmin (step up). These step changes are consistent with the results of Nicholls et al. (1996c) on the influence of the change from Glaisher stands to Stevenson screens. They found that Tmin recorded in a Glaisher stand was consistently around 0.2 °C cooler than that observed in a Stevenson screen, while Tmax observations were generally warmer in a Glaisher stand, with the greatest difference (up to 1 °C) recorded in austral summer. The adjustments applied to SEA38 appear to have minimised these step changes and associated biases due to the network-wide change of temperature screens at the beginning of the 20th century.

Small step changes of approximately 0.7 °C are still apparent for Tmax, Tmin and the DTR over 1908–1910, similar in size to other interannual temperature variations seen in the time series. This may mean that the effect of the screen changes has not been completely removed; however, it may also indicate the influence of prolonged La Niña event that occurred from September 1908–February 1911

Table 2. Temperature stations in SEA38 that did not have enough highly correlated neighbours for reference series development. Station numbers are given in brackets.

Tmax	*Tmin*
Brisbane (40842)	Kapunda (23007, 23321, 23373)
Yamba (58012)	Wilcannia (46043)
Gabo Island (84016)	Cobar (48030, 48027)
	Wollongong (68069, 68053, 68188, 68228)
	Mildura (76077,76031)
	Wilson's Promontory (85096)
	Gabo Island (84016)

Fig. 5. Number of adjustments made per decade for Tmax (black columns) and Tmin (white columns), 1860–1950. The column labels refer to the starting year of each decade. Note that 1940 refers to the 11-year period 1940–1950 inclusive.

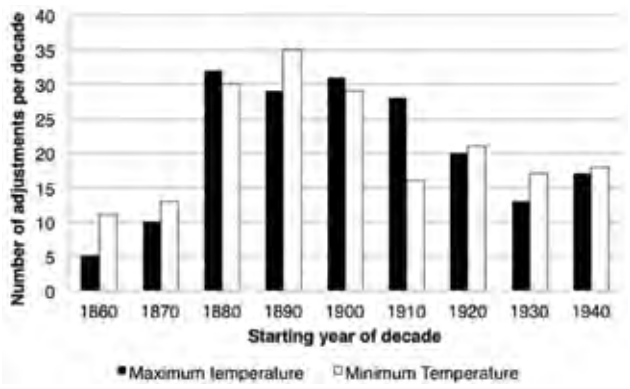

Fig. 6. Area-averaged SEA annual anomalies (°C, relative to the 1910–1950 base period) of original data from SEA38 (1860–1950, dashed line), adjusted data from SEA38 (1860–1950, solid red line) and data from ACORN–SAT49 over SEA (1910–1950, solid blue line) for (a) Tmax, (b) Tmin and (c) DTR, 1860–1950. The maximum and minimum anomalies for each year across the network are also plotted for the original SEA38 data (grey shading with black outline), adjusted SEA38 data (pink shading with red outline) and ACORN–SAT49 data (blue dotted lines).

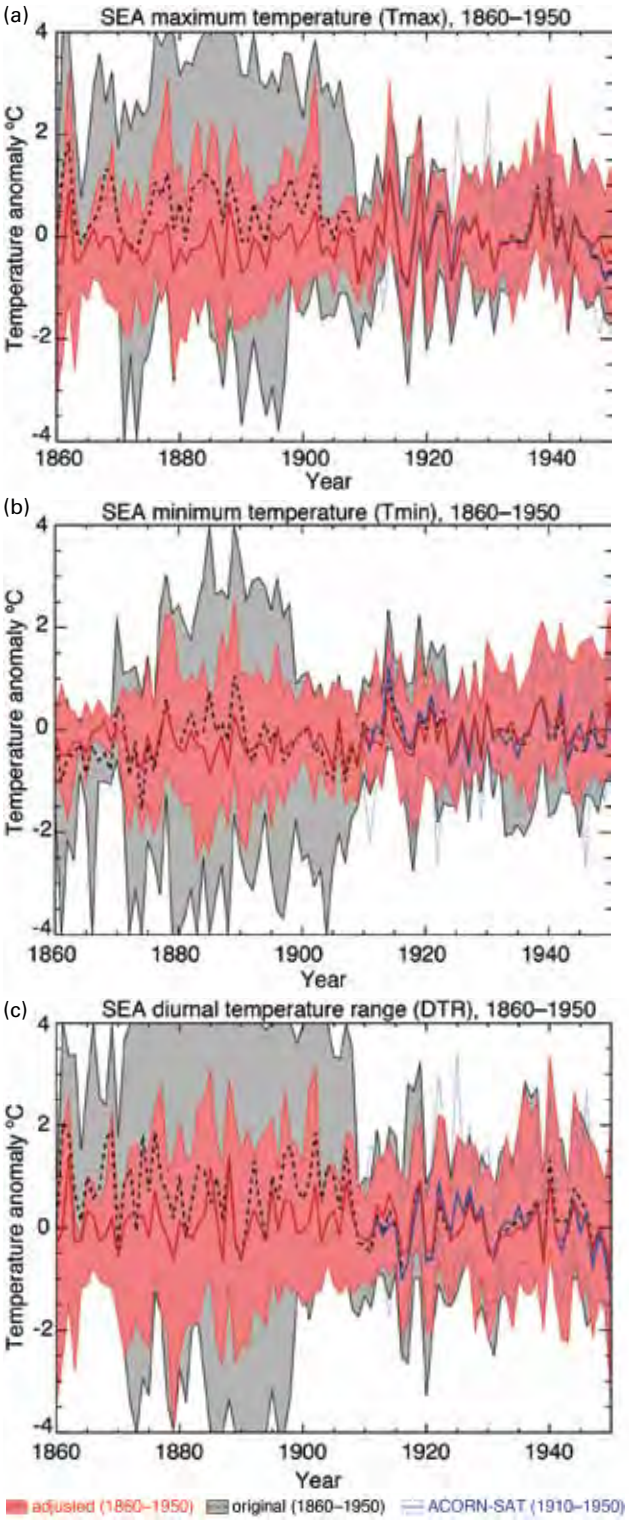

(Gergis and Fowler 2005; Australian Bureau of Meteorology 2011) causing negative anomalies in Tmax and the DTR, and positive Tmin anomalies (Power et al. 1998). Temperature variations in the 1880s also appear to be associated with ENSO phases, adding credence to this possibility. A fall in Tmax and DTR values and a corresponding rise in Tmin were observed during 1887 and 1889–1890, when a La Niña event was recorded in the SOI and Niño 3.4 index. Conversely, El Niño or neutral conditions were associated with an increase in Tmax and DTR values during 1883–1885 and 1888, while a decrease in Tmin values was recorded for the same time periods.

Figure 8 shows the annual area-averaged Tmax, Tmin and DTR from 1860–2011 together to enable an easier examination of coherent temperature variations over the past 152 years. The area-average of SEA38 and ACORN–SAT49 have been combined using the constant-difference method to produce a single temperature series for SEA from 1860–2011. Focusing on 1860–1909 reveals a synchronous cooling of Tmax and Tmin over 1872–1875 and 1891–1894, as well as a period of high interannual variation in Tmax, Tmin and the DTR from 1885–1890. This is similar to the 1914–1920 period when large year-to-year changes in temperature, particularly Tmax, can be seen. The years 1862, 1878, 1885, 1888, 1898 and 1902 are characterised by an increase in Tmax, while 1868, 1878, 1882, 1887 and 1889 show in increase in Tmin. Years that experienced a drop in Tmax include 1863, 1887, 1879 and 1881 and years of cool Tmin include 1862, 1885 and 1888. Preliminary analysis (not shown) suggests that years with above-average Tmax were associated with low amounts of rainfall, while years with above-

Fig 7. Standard deviations (°C) for annual anomalies (relative to the 1910–1950 base period) of Tmax (black), Tmin (medium grey) and DTR (light grey) in a 30-year moving window for original data (dashed line) and adjusted data (solid line) for SEA for 1860–2009, averaged over all stations in SEA38. Adjusted data from SEA38 (1860–1950) has been combined with data from the AWAP38 gridpoint data (1910–2009) using the constant-difference method to calculate the standard deviations for 1860–2009.

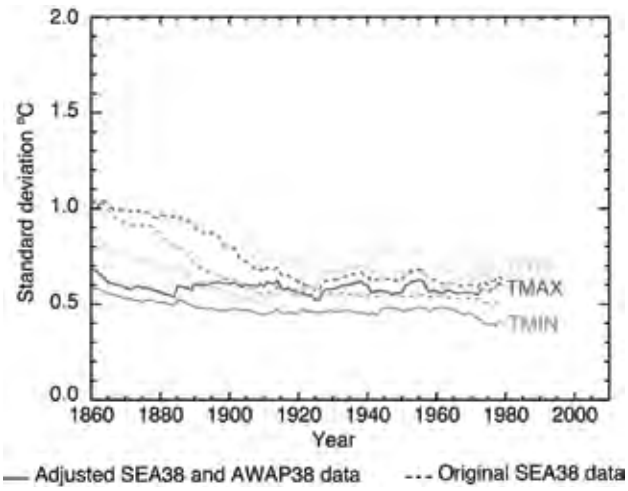

average Tmin experienced high rainfall. This association between temperature and rainfall agrees with the physical relationship outlined by Power et al. (1998), strengthening the validity of the temperature variations identified using the adjusted network.

Temperature variations identified in the SEA area-average also agree well with those found in the individual station temperature series. This can be seen by a visual inspection of the individual series (not shown) and is shown by Fig. 9, which plots the correlation between each station record and the SEA area-average for (a) Tmax and (b) Tmin for 1860–1950. In general the correlations are fairly high, particularly for the maximum temperatures of inland stations such as Wilcannia. If these correlations are compared to the equivalent ACORN–SAT49 correlations over the 1910–2011 period (not shown), the spatial coherence is similar, even if the correlations for SEA38 are somewhat lower. Correlations between the area-average and coastal stations such as Wollongong and Gabo Island are lower than those inland. These did not undergo reference series adjustments, which may explain the lower correlations. The lower correlations could also be due to different processes affecting temperature on the eastern coast (Catto 2012).

One criticism of the homogenisation technique used in this analysis might be that with a two-stage adjustment process, the station data are somewhat 'geared' to correlate with the area-average in this way, particularly as one station can be involved with the reference series of many others due to the relatively small size of the station network. However, the number of stations used within each reference series was small (a maximum of five), and confined to the subregions surrounding the candidate station. We can therefore be more confident that the agreement between the area-average and the SEA38 stations across the network is reflecting genuine temperature variations in SEA.

Comparing SEA38 to ACORN–SAT49 for 1910–1950 in Table 3 reveals very high correlations, when considering both the seasonal and annual area-averages. Annual Tmax area-averages have correlation coefficients of 0.94, while the Tmin and DTR correlation coefficients are slightly lower at 0.85 and 0.84 respectively. All seasonal correlations are 0.9 or higher, with Tmax in particular displaying very good agreement with the high-quality ACORN–SAT49 data. Very similar results were obtained by comparing the SEA38 area-average with the AWAP38 gridpoint network average (not shown).

Disagreements between the annual SEA38 and ACORN–SAT49 Tmax are confined to the 1940–1950 period (see Fig. 6a), possibly due to the movement of many stations from town centres to regional airports during the 1940s as aviation meteorology became more important (Torok and Nicholls 1996; Trewin 2012). The disagreements may also be caused by issues in the identification of changepoints at the end of the series (Wang et al. 2007; Wang 2008a). Discrepancies between the Tmin and DTR series from SEA38 and ACORN–SAT49 are primarily in the 1910–1920 period (Fig. 6(b) and

Fig. 8. Area-average annual anomalies (°C, relative to the 1910–1950 base period) of Tmax (top, solid line), Tmin (middle, dashed line) and DTR (bottom, dotted and dashed line) for SEA over 1860–2011. Adjusted data from SEA38 (1860–1950) has been combined with data from ACORN–SAT49 (1910–2011) using the constant-difference method to provide an adjusted dataset for 1860–2011.

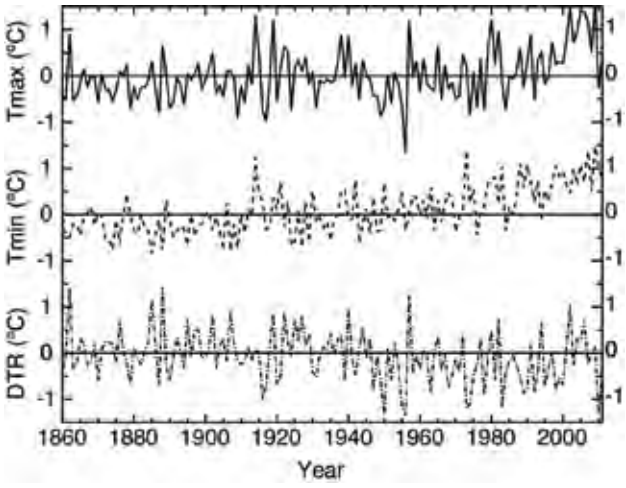

Fig. 9. Pearson correlation coefficients (multiplied by 100) between annual temperature anomalies (relative to the 1910–1950 base period) at each station in SEA38 and the SEA38 area-average over 1860–1950 for (a) Tmax and (b) Tmin.

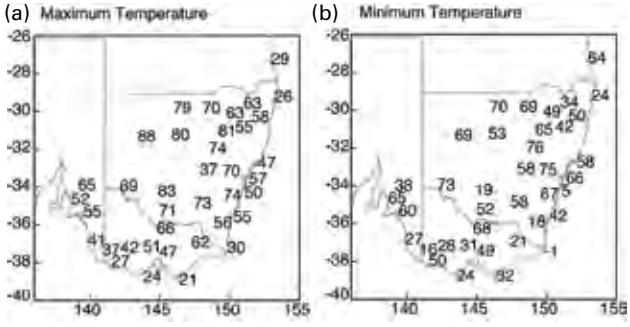

Table 3. Correlations between annual and seasonal ACORN–SAT49 and SEA38 area-averaged data, 1910–1950. Austral summer is represented by DJF (December–February), autumn by MAM (March–May), winter by JJA (June–August) and spring by SON (September–November). All correlations are significant at the five per cent level ($r \geq 0.30$ by a two-tailed student's t test with 41 independent samples).

	Annual	*DJF*	*MAM*	*JJA*	*SON*
Tmax	0.94	0.96	0.96	0.98	0.98
Tmin	0.85	0.91	0.92	0.94	0.92
DTR	0.84	0.90	0.94	0.95	0.93

Fig 6(c)), with SEA38 reporting lower values of Tmin and therefore higher DTR values. These differences may be a result of the ACORN–SAT homogenisation process being conducted on daily and monthly data (Trewin 2012) allowing for a greater identification of extremes and large Tmin anomalies like the one seen in 1914. However, all of these differences are small (less than 0.5 °C), and the interannual variability of both ACORN–SAT and SEA38 over the 1910–1950 period is very similar.

Overall, the adjustment process has improved the quality of the 1860–1950 SEA temperature record by reducing the data variability across SEA38 and minimising the influence of a network-wide change of thermometer screens at the start of the 20th century. Adjusted data from a small number of coastal stations (e.g. Wollongong and Gabo Island) exhibit low correlations with the adjusted area-average so should be interpreted cautiously. The majority of stations, however, show an improvement in data quality over 1860–1909, with a large number of clear step changes and unrealistic data adjusted to values comparable to the ACORN–SAT high-quality temperature data currently used for Australian climate research. The data variability has been reduced to a range similar to the ACORN–SAT stations across SEA, and the correlations between the adjusted network area-average and the annual and seasonal values from modern observational and gridded datasets are very high for the overlapping period ($r \approx 0.9$). This is an encouraging result considering that the homogenisation approaches used in developing the ACORN–SAT and AWAP datasets were quite different from that used in this study (Jones et al. 2009; Trewin 2012).

Southeastern Australian temperature, 1860–2011: links to ENSO, the IPO and long-term trends

Having assessed the quality of the extended temperature record, we now examine the relationship between SEA temperature variability and ENSO from 1876–2011. Table 4 shows the annual and seasonal correlations between the SOI and Niño 3.4 index and Tmax, Tmin and the DTR over the 1876–2011 period. Niño 3.4 correlations were multiplied by –1 to aid comparison. May–April annual means were used in the annual analysis to capture peak covariability between SEA climate and ENSO (Risbey et al. 2009b; Gergis et al. 2012a).

Correlations between SEA temperature and SOI and SEA temperature and the Niño 3.4 index are very similar. Significant correlations are evident between the annual (May–April) ENSO phase and Tmax was well as ENSO and the DTR for 1876–2011. A non-significant positive relationship is also apparent between annual Tmin values and ENSO. These relationships are similar to those identified by identified by Power et al. (1998) for the 1910–1992 period. Seasonal relationships shown in Table 4 reveal high correlations between ENSO and Tmax for all seasons apart from austral autumn, a known season of low ENSO–SEA influence (McBride and Nicholls 1983; Murphy and Timbal 2008). The DTR–ENSO correlations are similar to those for Tmax. ENSO–Tmin correlations are only significant during the austral winter. These results are in contrast to Jones and Trewin (2000), who also found a significant correlation between ENSO and SEA Tmin during autumn.

An additional 49 years of temperature data also allows for a longer examination of the temporal variability in the ENSO–SEA temperature relationship. Figure 10 shows 13-year moving correlations between the SOI and Tmax, Tmin and the DTR for austral summer, winter and May–April annual means. Very similar results were obtained using the Niño 3.4 index (not shown). Thirteen years was chosen as the time period to identify the decadal signal common to the smoothed IPO time series. There are clear variations in the strength of the SOI–temperature relationships, with times of weakened and even reversed correlation values in the 1890–1900s, 1920–1930s and 1960–1970s for Tmax, Tmin and the DTR. During these periods, the negative correlations between the SOI and Tmax and the DTR reduce or become positive, and the positive correlations between the SOI and Tmin become negative.

Annual and austral winter variations appear largely in-phase for all variables but austral summer variations are somewhat different, particularly for Tmin and the DTR. The spatial correlation patterns calculated by Jones and Trewin (2000a) for 1950–1994 identified a high-level of spatial variability in the austral summer ENSO–temperature relationship across SEA. Positive correlations were identified across Victoria and eastern South Australia, while negative correlations were widespread across most of New South Wales and southern Queensland (Jones and Trewin 2000, Fig. 4). Thus the weaker correlations across SEA in summer found in this study may reflect the area-averaging of correlations of opposing signs across the region. Fluctuations in the Australian temperature–ENSO relationship have previously been recognised in similar post-1900 periods in other studies (Lough 1997 for Queensland; Power et al. 1999a for Australia). The new temperature data for 1860–1909 has allowed for the identification of another period of weakened correlations across the SEA region in the late 19th century.

Variations in the IPO may be one reason for the regional temperature fluctuations reported here. Power et al. (1999a) found that negative phases of the IPO were associated with higher correlations between the SOI and Australian Tmax, while positive IPO phases were linked to a great weakening in the Tmax–SOI relationship. Indeed, average correlations between ENSO and each temperature variable for 1876–2009 over SEA during both phases of the IPO, given in Table 5, supports the Power et al. (1999a) findings for all-Australian data. Table 5 shows that correlations are larger between ENSO (represented by the SOI and the Niño 3.4 index) and SEA temperature when the IPO is negative, compared to years when the IPO is positive. But it is clear from the 13-year running correlations shown in Fig. 10 that there is large variability in this relationship. Correlations between May–

Table 4. Correlations between the SOI and the Niño 3.4 index and area-averaged SEA Tmax, Tmin and DTR for May–April annual, austral summer (DJF), autumn (MAM), winter (JJA) and spring (SON) area-averages from 1876–2011. Niño 3.4 correlations are given in brackets and are multiplied by –1 for comparison. Values printed in bold are statistically significant at the five per cent level (r ≥ 0.195 by a two-tailed student's *t* test with 135 independent samples).

	May–April ANN	*DJF*	*MAM*	*JJA*	*SON*
Tmax	**–0.42 (–0.39)**	**–0.26 (–0.37)**	–0.14 (–0.11)	**–0.30 (–0.22)**	**–0.34 (–0.37)**
Tmin	0.07 (0.02)	–0.03 (–0.18)	0.05 (–0.04)	**0.34 (–0.21)**	0.05 (0.00)
DTR	**–0.51 (–0.50)**	**–0.29 (–0.26)**	–0.18 (–0.06)	**–0.51 (–0.35)**	**–0.47 (–0.47)**

Table 5. Correlations between the SOI and Niño 3.4 index and the area-averaged SEA Tmax, Tmin and DTR for May–April annual, DJF and JJA means from 1876–2011 when the IPO is positive (> 0.5) and negative (< –0.5). The number of years for each IPO phase is given in brackets in the left hand column. Niño 3.4 correlations are given in brackets and are multiplied by –1 for comparison. Values printed in bold are statistically significant at the five per cent level (r ≥ 0.25 by a two-tailed student's *t* test with 58 independent samples for the positive IPO phase, r ≥ 0.28 by a two-tailed student's *t* test with 48 independent samples for the negative IPO phase).

	Annual Tmax	*Annual Tmin*	*Annual DTR*	*DJF Tmax*	*DJF Tmin*	*DJF DTR*	*JJA Tmax*	*JJA Tmin*	*JJA DTR*
Positive IPO (58 years)	**–0.26 (–0.33)**	0.06 (–0.01)	**–0.28 (–0.33)**	–0.01 (–0.16)	0.01 (–0.17)	–0.02 (–0.02)	**–0.39** (–0.23)	0.26 (0.19)	**–0.47 (–0.33)**
Negative IPO (46 years)	**–0.57 (–0.56)**	0.02 (–0.12)	**–0.64 (–0.54)**	**–0.47 (–0.59)**	–0.11 **(–0.34)**	**–0.42 (–0.32)**	**–0.37** (–0.27)	**0.48** (0.20)	**–0.60 (–0.34)**

Table 6. Trends (°C per 50 years) of area-averaged SEA Tmax, Tmin and DTR for annual, austral summer (DJF) and winter (JJA) values calculated over the 50-year periods 1860–1909 and 1910–1959, the 52-year 1960–2011 period and the 152-year 1860–2011 period. Values printed in bold are statistically significant from zero, as determined by the student's *t* test distribution ($p < 0.05$).

	Tmax Ann	*Tmin Ann*	*DTR Ann*	*Tmax DJF*	*Tmin DJF*	*DTR DJF*	*Tmax JJA*	*Tmin JJA*	*DTR JJA*
1860–1909	0.06	–0.12	0.18	**0.69**	0.36	0.33	–0.08	–0.43	0.35
1910–1959	–0.31	0.00	–0.32	–0.33	–0.03	–0.31	–0.01	–0.10	0.09
1960–2011	**1.08**	**0.90**	0.19	**1.03**	**1.17**	–0.15	**1.08**	**0.89**	0.19
1860–2011	**0.22**	**0.37**	–0.15	**0.15**	**0.51**	–0.36	**0.41**	**0.23**	**0.18**

April Tmax and the SOI during negative phases of the IPO, for example, are seen to vary from around –0.8 in the 1950s to 0.05 during the 1890s (Fig. 10(a)). The period of highest correlations between Tmax and the SOI around 1910 is conversely associated with a strong positive phase of the IPO.

These results suggest that the modifying influence of the IPO on the relationship between regional SEA temperature and large-scale ENSO fluctuations may be more complicated than previously thought. Model studies have identified the possibility of a reversal in the relationship between the IPO and how ENSO influences the Australian climate (Arblaster et al. 2002). Additionally, the strength of a La Niña event is more linearly related to cool anomalies of Australian temperature and wet anomalies of Australian rainfall than the strength of an El Niño event is related to the size of warm temperature and dry rainfall anomalies in Australia (Power et al. 2006). This nonlinearity may have led to the higher correlations found by Power et al. (1999a) between ENSO and the Australian climate during negative IPO phases, as La Niña events are more prevalent during this phase (Kiem et al. 2003; Power et al. 2006; Parker et al. 2007). Decadal fluctuations of Indian Ocean sea surface temperatures may also be influencing the relationship between ENSO and SEA temperature, as the eastern Indian Ocean in particular plays a large role in the teleconnection between ENSO and SEA rainfall in austral spring (Cai et al. 2011).

Finally, the extended temperature record allows an examination of SEA temperature trends from 1860–2011. Table 6 shows the trends of the SEA38 and ACORN–SAT49 combined area-averaged Tmax, Tmin and the DTR in the 50-year periods of 1860–1909 and 1910–1959, the 52 year period of 1960–2011 as well as the full 1860–2011 period. The 1860–1909 period was characterised by insignificant trends of 0.06 °C and –0.12 °C in annual Tmax and Tmin. The only significant trend in the 1860–1909 period is for austral summer Tmax values. This may be due to some remaining inhomogeneities in the early data because non-standard thermometer exposure can have a greater impact on summer Tmax values than other observations (Nicholls et al. 1996c). The 1910–1959 period experienced an insignificant cooling trend of –0.31 °C in Tmax and no trend in Tmin. Small negative trends are seen in the DTR in summer for most of the 20th century, and positive trends observed in austral winter, although they are largely insignificant.

Fig. 10. Moving 13-year correlations between the Southern Oscillation Index (SOI) and SEA38 area-averaged (a) Tmax, (b) Tmin, and (c) DTR for May–April annual (solid line), austral summer (December–February, DJF, dotted line) and austral winter (June–August, JJA, dashed line), 1876–2009. Annual IPO values for 1876–2009 are also plotted (grey shading) after being smoothed using an 11-year Chebyshev filter. Correlations greater than ±0.51 (dotted horizontal lines) are statistically significant at the five per cent level, as determined by the two-tailed student's *t* test ($p < 0.05$ for 13 independent samples).

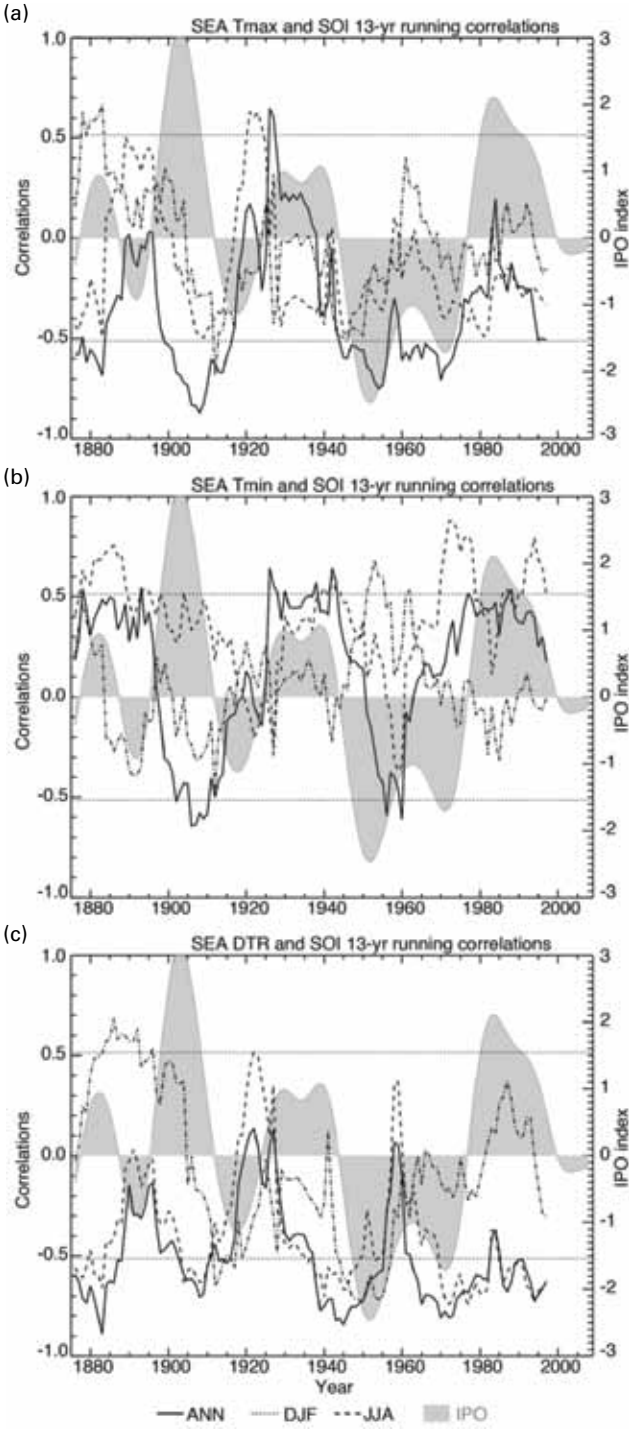

The recent 1960–2011 period is dominated by positive trends that are statistically significant. Increases in Tmax and Tmin are observed both annually and in austral summer and winter from 1960–2011. Positive Tmax trends are larger than Tmin trends for the recent 1960–2011 period, with a warming of 1.12 °C in the last 52 years for Tmax (1.08 °C per 50 years) compared to 0.94 °C for Tmin (0.90 °C per 50 years). These findings are in agreement with SEA temperature trends found by Murphy and Timbal (2008) since 1950. However, Tmin appears to be warming at a greater rate than Tmax over the full 1860–2011 period, with a significant positive trend of 0.37 °C per 50 years (or 1.1 °C over the whole 152 years), compared to 0.22 °C per 50 years (0.67 °C over 1860–2011).

The absolute trend values over the 1860–1909 and 1860–2011 periods must be treated with some caution, due to possible remaining inhomogeneities and the reduced spatial network over 1860–1870. Trend analysis conducted on the area-average of 12 SEA temperature stations with data beginning in 1860–1869 produced non-significant negative trends in Tmax and Tmin for 1869–1909. It also returned a larger trend in Tmax and a smaller trend in Tmin over the full 1860–2011 period than trend analysis conducted on the full SEA38 area-average. However, the 1860–2011 trends in Tmax and Tmin were still positive and highly significant, further supporting the conclusion drawn from Table 6 that the vast majority of warming in the SEA region has occurred since 1960. These trends also agree with current research on temperature trends Australia-wide, indicating that Tmin values are warming faster than Tmax, and that the majority of warming has occurred in the last 50–60 years (CSIRO and the Australian Bureau of Meteorology 2012).

Conclusions

A network of 38 long-term temperature stations from SEA was developed to give the first detailed picture of temperature variations in the region over the 1860–1909 period. Non-climatic discontinuities, including the influence of a network wide change from non-standard thermometer enclosures to Stevenson screens at the start of the 20th century, were identified and minimised. This was achieved using a novel two-step process, which combined statistical techniques and station history information to identify changepoints in individual station data and then changepoints relative to constructed reference series.

The two-stage homogenisation process resulted in large improvements in the coherence and quality of seasonal and annual pre-1910 temperature data across SEA38. The variability of the temperature data before 1910 was greatly reduced, making it directly comparable with observations used in modern climate research. The correlations between the adjusted temperature dataset and the high-quality observational and gridded temperature datasets available were very high ($r \approx 0.9$) for both annual and seasonal data in the 1910–1950 period of overlap.

Combining the 1860–1950 data with the high-quality ACORN–SAT data for SEA over 1910–2011 allowed the first examination of temperature variations in SEA over the past 152 years. The relationships identified between the SOI and SEA temperature from 1860–2011 are similar to those found using 20th century data alone (Power et al. 1998; Jones and Trewin 2000), showing the ability of the adjusted dataset to capture known SEA temperature features. Low-frequency variations in the ENSO–temperature relationship were similar to those found for other parts of Australia and an additional period of weak correlations in the 1890s was identified using the new SEA38 dataset.

Our results suggest that changes in the way ENSO influences SEA temperature are not linked to a particular phase of the IPO and further research should be targeted at determining whether there is another physical explanation or low-frequency circulation that may be driving these changes. Cai et al. (2011) have recently identified the dominant influence of eastern Indian Ocean sea surface temperatures in the teleconnection between ENSO and SEA rainfall, particularly in the austral spring, through Rossby wave formation. This important interplay between Pacific and Indian Ocean temperature and how these tropical processes affect SEA temperature is the topic of current research.

Periods of cool Tmax and Tmin were identified during 1872–1875 and 1891–1894, while warmer Tmax and Tmin were recorded around 1878. High interannual variability dominated the Tmax and Tmin record during 1885–1890. The 1860–1909 and 1910–1959 periods were characterised by insignificant trends in annual Tmax and Tmin. The recent 1960–2011 period on the other hand was dominated by positive trends of 1.12 °C and 0.93 °C in Tmax and Tmin respectively, leading to significant warming identified over the full 1860–2011 period. The 1960–2011 trends found in this study are in agreement with previous research on SEA temperature, and the additional 49 years of temperature data show that temperature increases in SEA since 1960 are the largest and most significant over the past 152 years.

A new historical temperature dataset for SEA presents further opportunities to research long-term variations of climate across the country's most highly populated region. Forthcoming work will explore the relationship between ENSO and SEA temperature, pressure and rainfall in the mid 19th and early 20th centuries, to provide improved insight into the fundamental relationships that influence SEA climate variability.

The extension of the SEA temperature record also provides an opportunity for extended data to calibrate and validate palaeoclimate reconstructions (Gergis et al. 2012a; Gergis et al. in review). Given that there are few sources of early instrumental data for Australia compared to other countries around the world (Nicholls et al. 2006), the development of this extended temperature record is an important step in improving data availability for SEA climate research.

Acknowledgements

This research is funded by an Australian Research Council (ARC) Linkage Project (LP0990151). Many thanks to staff at the National Meteorological Library, the National Archives of Australia and the Australian Bureau of Meteorology Climate Data Management and Record Management groups for their patience and assistance in locating station metadata. Particular thanks go to Clive Brett, Meaghan Flannery, Cris Gouletsas, Karen Rowney and Karl Braganza. Thanks also to Blair Trewin and two anonymous reviewers for their helpful advice, which improved this manuscript. Research space was kindly provided by the Australian Bureau of Meteorology National Climate Centre and Climate Data Management groups.

References

Aguilar, E., Auer, I., Brunet, M., Peterson, T.C. and Wieringa, J. 2003. *Guidelines on Climate Metadata and Homogenization*. World Meteorological Organization, Geneva, 51 pp.

Alexander, L.V., Hope, P., Collins, D., Trewin, B., Lynch, A. and Nicholls, N. 2007. Trends in Australia's climate means and extremes: a global context. *Aust. Meteorol. Mag., 56*, 1–18.

Alexander, L.V., Uotila, P., Nicholls, N. and Lynch, A. 2010. A new daily pressure dataset for Australia and its application to the assessment of changes in synoptic patterns during the last century. *J. Clim., 23,* 1111–26.

Alexandersson, H. 1986. A homogeneity test applied to precipitation data. *J. Clim., 6,* 661–75.

Arblaster, J., Meehl, G.M. and Moore, A.M. 2002. Interdecadal modulation of Australian rainfall. *Clim. Dyn., 18*, 519–31, doi: 10.1007/s00382-001-0191-y.

Australian Bureau of Meteorology. 1997. *Guidelines for the Siting and Exposure of Meteorological Instruments and Observing Facilities*. Bureau of Meteorology, Melbourne, 92 pp.

Australian Bureau of Meteorology. 2000. Australian Data Archive for Meteorology. Climate Data Online. Available online at http://www.bom.gov.au/climate/cdo/images/about/ADAM.pdf

Australian Bureau of Meteorology, cited 2010. Bureau of Meteorology Rainfall Districts. Available online at www.bom.gov.au/climate/cdo/about/rain-districts.shtml

Australian Bureau of Meteorology, cited 2011. Southern Oscillation Index (SOI) Archives. Available online at http://reg.bom.gov.au/climate/current/soihtm1.shtml

Australian Bureau of Meteorology, cited 2012a. Australian climate variability and change: Annual Mean Temperature Anomaly—Southeastern Australia. Available online at www.bom.gov.au/cgi-bin/climate/change/timeseries.cgi?graph=tmean&area=seaus&season=0112&ave_yr=0

Australian Bureau of Meteorology, cited 2012b. *The Australian Climate Observations Reference Network—Surface Air Temperature (ACORN–SAT): Observation practises*. Australian Bureau of Meteorology, Melbourne, 30 pp.

Australian Bureau of Statistics, cited 2011. Australian Demographic Statistics, March 2011. Available online at www.abs.gov.au

Barring, L., Jonsson, P., Achberger, C., Ekstrom, M. and Alexandersson, H. 1999. The Lund instrumental record of meteorological observations: Reconstruction of monthly sea-level pressure 1780–1997. *Int. J. Climatol., 19,* 1427–43.

Brunetti, M., Maugeri, M., Monti, F. and Nanni, T. 2006. Temperature and precipitation variability in Italy in the last two centuries from homogenised instrumental time series. *Int. J. Climatol., 26,* 345–81, doi: 10.1002/joc.1251.

Cai, W. and van Rensch, P. 2012. The 2011 southeast Queensland extreme summer rainfall: A confirmation of a negative Pacific Decadal Oscillation phase? *Geophys. Res. Lett., 39,* L08702, doi: 10.1029/2011GL050820.

Cai, W., van Rensch, P. and Cowan, T. 2011. Teleconnection pathways of ENSO and the IOD and the mechanisms for impacts on Australian rainfall. *J. Clim., 24,* 3910–23.

Catto, J. 2012. When is it hottest in Victoria? *Bull. Aust. Met. Oceanogr. Soc., 25*, 63–7.

Conrad, V. and Pollak, C. 1950. *Methods in Climatology*. Harvard University Press, Cambridge, 459 pp.

Cornes, R.C., Jones, P.D., Briffa, K.R. and Osborn, T.J. 2012. A daily series of mean sea-level pressure for London, 1692–2007. *Int. J. Climatol, 32,* 641–56, doi: 10.1002/joc.2301.

CSIRO and the Australian Bureau of Meteorology. 2012. *State of the Climate 2012,* 8 pp. Available online at http://www.csiro.au/resources/State-of-the-Climate.html

Day, D. 2007. *The Weather Watchers: 100 years of the Bureau of Meteorology*. Melbourne University Publishing, 530 pp.

DeGaetano, A.T. 2006. Attributes of several methods for detecting discontinuities in mean temperature series. *J. Clim., 19,* 838–53, doi: 10.1175/JCLI3662.1.

Della-Marta, P., Collins, D. and Braganza, K. 2004. Updating Australia's high-quality annual temperature dataset. *Aust. Meteorol. Mag., 53,* 75–93.

Douglas, K. 2007. Under such sunny skies: understanding weather in colonial Australia, 1860–1901. *Metarch Papers No. 17*. Bureau of Meteorology, Melbourne, 54 pp.

Ducrè-Robitaille, J.F., Vincent, L.A. and Boulet, G. 2003. Comparison of techniques for detection of discontinuities in temperature series. Int. *J. Climatol., 23,* 1087–101, doi: 10.1002/joc.924.

Easterling, D.R. and Peterson, T.C. 1995. A new method for detecting undocumented discontinuities in climatological time series. *Int. J. Climatol., 15,* 369–77, doi: 10.1002/joc.3370150403.

Easterling, D.R., Peterson, T.C. and Karl, T.R. 1996. On the development and use of homogenized climate datasets. *J. Clim., 9,* 1429–34.

ETCCDI, cited 2009. The Joint CCI/CLIVAR/JCOMM Expert Team (ET) on Climate Change Detection and Indices (ETCCDI). Available online athttp://cccma.seos.uvic.ca/ETCCDMI/

Fawcett, R., Trewin, B., Braganza, K., Smalley, R.J., Jovanovic, B. and Jones, D.A. 2012. On the sensitivity of Australian temperature trends and variability to analysis methods and observation networks. *CAWCR Technical Report No. 50*. CSIRO and the Australian Bureau of Meteorology, Melbourne, 54 pp.

Folland, C. 2008. Climate of the 20th Century: IPO Time Series. Available online at www.iges.org/c20c/IPO_v2.doc

Folland, C.K., Renwick, J.A., Salinger, M.J. and Mullan, A.B. 2002. Relative influences of the Interdecadal Pacific Oscillation and ENSO on the South Pacific Convergence Zone. *Geophys. Res. Lett., 29,* 1643, doi: 10.1029/2001gl014201.

Folland, C., Parker, D., Colman, A. and Washington, R. 1997. Large scale modes of ocean surface temperature since the late nineteenth century. *Beyond El Niño: Decadal and interdecadal climate variability,* A. Navarra, Ed. Springer, Berlin, 73–102.

Gentilli, J. 1967. A history of meteorological and climatological studies in Australia. *University Studies in History, 5*, 54–88.

Gergis, J.L. and Fowler, A.M. 2005. Classification of synchronous oceanic and atmospheric El Niño-Southern Oscillation (ENSO) events for palaeoclimate reconstruction. *Int. J. Climatol., 25,* 1541–65, doi: 10.1002/joc.1202.

Gergis, J., Gallant, A., Braganza, K., Karoly, D.J., Allen, K., Cullen, L., D'Arrigo, R., Goodwin, I., Grierson, P. and McGregor, S. 2012a. On the long-term context of the 1997–2009 'Big Dry' in south-eastern Australia: insights from a 206-year multi-proxy rainfall reconstruction. *Clim. Change, 111*, 923–44, doi: 10.1007/s10584-011-0263-x.

Gergis, J., Neukom, R., Gallant, A. and Aus2K members, in review. Evidence of rapid late C20th warming from an Australasian temperature reconstruction spanning the last millennium. *J. Clim.,* in review.

Hasson, A., Mills, G., Timbal, B. and Walsh, K. 2009. Assessing the impact of climate change on extreme fire weather events over southeastern Australia. *Clim. Res., 39*, 159–72.

Jones, D.A. 1999. Characteristics of Australian land surface temperature variability. *Theor. Appl. Climatol., 63,* 11–31, doi: 10.1007/s007040050088.

Jones, D.A. and Trewin, B. 2000. On the relationships between the El Niño–Southern Oscillation and Australian land surface temperature. *Int. J. Climatol., 20,* 697–719, doi: 10.1002/1097-0088.

Jones, D.A., Wang, W. and Fawcett, R. 2009. High-quality spatial climate data-sets for Australia. *Aust. Meteorol. Oceanogr. J., 58,* 233–48.

Jones, P. 1991. Historical records of cloud cover and climate for Australia. *Aust. Meteorol. Mag., 39,* 181–89.

Jones, P.D., Lister, D.H., Osborn, T.J., Harpham, C., Salmon, M. and Morice, C.P. 2012. Hemispheric and large-scale land-surface air temperature variations: An extensive revision and an update to 2010. *J. Geophys. Res., 117,* doi: 10.1029/2011JD017139.

Karoly, D.J. and Braganza, K. 2005. Attribution of recent temperature changes in the Australian region. *J. Clim., 18,* 457–64, doi: 10.1175/JCLI-3265.1.

Kestin, T.S., Karoly, D.J., Yano, J.-I. and Rayner, N.A. 1998. Time-frequency variability of ENSO and stochastic simulations. *J. Clim., 11,* 2258–72, doi: 10.1175/1520-0442.

Kiem, A.S., Franks, S.W. and Kuczera, G. 2003. Multi-decadal variability of flood risk. *Geophys. Res. Lett., 30,* 1035, doi: 10.1029/2002GL015992.

Lavery, B., Joung, G. and Nicholls, N., 1997. An extended high-quality historical rainfall dataset for Australia. *Aust. Meteorol. Mag., 46,* 27–38.

Lough, J.M. 1997. Regional indices of climate variation: temperature and rainfall in Queensland, Australia. *Int. J. Climatol., 17,* 55–66, doi: 10.1002/1097-0088.

Lund, R. and Reeves, J. 2002. Detection of undocumented changepoints: a revision of the two-phase regression model. *J. Clim., 15,* 2547–54, doi: 10.1175/1520-0442.

Mantua, N.J., Hare, S.R., Zhang, Y., Wallace, J.M. and Francis, R.C. 1997. A Pacific interdecadal climate oscillation with impacts on salmon production. *Bull. Am. Meteorol. Soc., 78,* 1069–79, doi: 10.1175/1520-0477.

McBride, J. and Nicholls, N. 1983. Seasonal relationships between Australian rainfall and the Southern Oscillation. *Mon. Weather Rev., 111,* 1998–2004.

Menne, M.J. and Williams, C.N. 2009. Homogenization of temperature series via pairwise comparisons. *J. Clim., 22,* 1700–17, doi: 10.1175/2008JCLI2263.1.

Moyal, A. 1986. *A bright & savage land: Scientists in colonial Australia*. Collins, Sydney, 240 pp.

Murphy, B. and Timbal, B. 2008. A review of recent climate variability and climate change in southeastern Australia. *Int. J. Climatol., 28,* 859–79.

Murray-Darling Basin Authority, cited 2011. About the Murray Darling Basin. [Available online at http://www.mdba.gov.au/explore-the-basin/about-the-basin].

Nicholls, N., Drosdowsky, W. and Lavery, B. 1996a. Australian rainfall variability and change. *Weather, 52,* 66–72.

Nicholls, N., Lavery, B., Frederiksen, C., Drosdowsky, W. and Torok, S. 1996b. Recent apparent changes in relationships between the El Niño Southern Oscillation and Australian rainfall and temperature. *Geophys. Res. Lett., 23,* 3357–60, doi: 10.1029/96gl03166.

Nicholls, N., Tapp, R., Burrows, K. and Richards, D. 1996c. Historical thermometer exposures in Australia. *Int. J. Climatol., 16,* 705–10.

Nicholls, N., Collins, D., Trewin, B. and Hope, P. 2006. Historical instrumental climate data for Australia—quality and utility for palaeoclimatic studies. *J. Q. Sci., 21,* 681–88.

Parker, D.E. 1994. Effects of changing exposure of thermometers at land stations. *Int. J. Climatol., 14,* 1–31.

Parker, D., Folland, C., Scaife, A., Knight, J., Colman, A., Baines, P. and Dong, B. 2007. Decadal to multidecadal variability and the climate change background. *J. Geophys. Res., 112,* D18115, doi: 10.1029/2007jd008411.

Peterson, T.C. and Easterling, D.R. 1994. Creation of homogenous composite climatological reference series. *Int. J. Climatol., 14,* 671–79.

Peterson, T.C., Easterling, D.R., Karl, T.R., Groisman, P., Nicholls, N., Plummer, N., Torok, S., Auer, I., Boehm, R., Gullett, D., Vincent, L., Heino, R., Tuomenvirta, H., Mestre, O., Szentimrey, T., Salinger, J., Forland, E.J., Hassen-Bauer, I., Alexandersson, H., Jones, P. and Parker, D. 1998. Homogeneity adjustments of in situ atmospheric climate data: a review. *Int. J. Climatol., 18,* 1493–517.

Pezza, A.B., van Rensch, P. and Cai, W. 2011. Severe heat waves in Southern Australia: synoptic climatology and large scale connections. *Clim. Dyn., 38,* 209–24, doi: 10.1007/s00382-011-1016-2.

Power, S., Tseitkin, F., Torok, S.J., Lavery, B., Dahni, R. and McAveny,

B. 1998. Australian temperature, Australian rainfall and the Southern Oscillation, 1910–1992: coherent variability and recent changes. *Aust. Meteorol. Mag., 47,* 85–101.

Power, S., Casey, T., Folland, C. and Colman, A. 1999a. Inter-decadal modulation of the impact of ENSO on Australia. *Clim. Dyn., 15,* 319–24.

Power, S., Tseitkin, F., Mehta, V., Lavery, B., Torok, S. and Holbrook, N. 1999b. Decadal climate variability in Australia during the twentieth century. *Int. J. Climatol., 19,* 169–84, doi: 10.1002/1097-0088.

Power, S., Haylock, M., Colman, R. and Wang, X.D. 2006. The predictability of interdecadal changes in ENSO activity and ENSO teleconnections. *J. Clim., 19,* 4755–71, doi: 10.1175/jcli3868.1.

Rayner, N.A., Parker, D.E., Horton, E.B., Folland, C.K., Alexander, L.V., Rowell, D.P., Kent, E.C. and Kaplan, A. 2003. Global analyses of sea surface temperature, sea ice, and night marine air temperature since the late nineteenth century. *J. Geophys. Res., 108,* 4407, doi: 10.1029/2002jd002670.

Reason, C.J.C., Allan, R.J. and Lindesay, J.A. 1998. Climate variability on decadal time scales: mechanisms and implications for climate change. *Palaeoclimates, 3,* 25–49.

Reeves, J., Chen, J., Wang, X.L., Lund, R. and Lu, Q.Q. 2007. A review and comparison of changepoint detection techniques for climate data. *J. Appl. Meteor. Climatol., 46,* 900–15, doi: 10.1175/JAM2493.1.

Reynolds, R.W. and Smith, T.M. 1994. Improved global sea surface temperature analyses using optimum interpolation. *J. Clim., 7,* 929–48.

Rhoades, D.A. and Salinger, M.J. 1993. Adjustment of temperature and rainfall records for site changes. *Int. J. Climatol., 13,* 899–913.

Risbey, J.S., Pook, M.J., McIntosh, P.C. Ummenhofer, C.C. and Meyers, G., 2009a. Characteristics and variability of synoptic features associated with cool season rainfall in southeastern Australia. *Int. J. Climatol., 29,* 1595–613, doi: 10.1002/joc.1775.

Risbey, J.S., Pook, M.J., McIntosh, P.C. Wheeler, M.C. and Hendon, H.H., 2009b. On the remote drivers of rainfall variability in Australia. *Mon. Weather Rev., 137,* 3233–53.

Slonosky, V.C. and Graham, E., 2005. Canadian pressure observations and circulation variability: links to air temperature. *Int. J. Climatol., 25,* 1473–92.

Street, R.B., Allsop, D. and Durocher, Y., 2007. *Guidelines for Managing Changes in Climate Observation Programmes*. World Meteorological Organization, Geneva, 24 pp.

Thiessen, A.H., 1911. Precipitation averages for large areas. *Mon. Weather Rev., 39,* 1082–89, doi: 10.1175/1520-0493.

Timbal, B. and Fawcett, R., 2012. A historical perspective on south-eastern Australia rainfall since 1865 using the instrumental record. *J. Clim.,* early issue, doi: 10.1175/JCLI-D-12-00082.1.

Torok, S., 1996. The development of a high quality historical temperature data base for Australia. PhD thesis, University of Melbourne, 229 pp.

Torok, S. and Nicholls, N., 1996. A historical annual temperature dataset for Australia. *Aust. Meteorol. Mag., 45,* 251–60.

Trenberth, K.E., 1997. The definition of El Niño. *Bull. Am. Meteorol. Soc., 78,* 2771–77, doi: 10.1175/1520-0477.

Trenberth, K.E. and Shea, D.J., 2005. Relationships between precipitation and surface temperature. *Geophys. Res. Lett., 32,* L14703.

Trenberth, K.E. and Stepaniak, D.P., 2001. Indices of El Niño evolution. *J. Clim., 14,* 1697–701.

Trenberth, K.E., Jones, P.D., Ambenje, P., Bojariu, R., Easterling, D., Klein Tank, A., Parker, D., Rahimzadeh, F., Renwick, J.A., Rusticucci, M., Soden, B. and Zhai, P., 2007. Observations: Surface and Atmospheric Climate Change. *Climate Change 2007: The Physical Science Basis. Contribution of Working Group I to the Fourth Assessment Report of the Intergovernmental Panel on Climate Change,* S. Solomonon et al., Eds., Cambridge University Press, Cambridge, United Kingdom and New York, NY, USA.

Trewin, B., 2010. Exposure, instrumentation, and observing practice effects on land temperature measurements. *Wiley Interdisciplinary Reviews: Climate Change, 1,* 490–506, doi: 10.1002/wcc.46.

Trewin, B., 2012. A daily homogenized temperature data set for Australia. *Int. J. Climatol.,* early issue, doi: 10.1002/joc.3530.

Ummenhofer, C.C., England, M.H., McIntosh, P.C., Meyers, G.A., Pook, M.J., Risbey, J.S., Gupta, A.S. and Taschetto, A.S., 2009. What causes southeast Australia's worst droughts? *Geophys. Res. Lett., 36,* L04706.

Ummenhofer, C.C., Gupta, A.S., Briggs, P.R., England, M.H., McIntosh, P.C., Meyers, G.A., Pook, M.J., Raupach, M.R. and Risbey, J.S., 2011. Indian and Pacific Ocean influences on southeast Australian drought and soil moisture. *J. Clim.,* 1313–36, doi: 10.1175/2010JCLI3475.1.

Venema, V.K.C., Mestre, O., Aguilar, E., Auer, I., Guijarro, J.A., Domonkos, P., Vertacnik, G., Szentimrey, T., Stepanek, P., Zahradnicek, P., Viarre, J., Müller-Westermeier, G., Lakatos, M., Williams, C.N., Menne, M., Lindau, R., Rasol, D., Rustemeier, E., Kolokythas, K., Marinova, T., Andresen, L., Acquaotta, F., Fratianni, S., Cheval, S., Klancar, M., Brunetti, M., Gruber, C., Prohom Duran, M., Likso, T., Esteban, P. and Brandsma, T., 2012. Benchmarking monthly homogenization algorithms for monthly data. *Clim. Past, 8,* 89–115, doi: 10.5194/cpd-7-2655-2011.

Verdon-Kidd, D.C. and Kiem, A.S., 2009. Nature and causes of protracted droughts in southeast Australia: Comparison between the Federation, WWII, and Big Dry droughts. *Geophys. Res. Lett., 36,* doi: 10.1029/2009GL041067.

Vincent, L.A., 1998. A technique for the identification of inhomogeneities in Canadian temperature series. *J. Clim., 11,* 1094–104.

Vincent, L.A. and Gullett, D.W., 1999. Canadian historical and homogeneous temperature datasets for climate change analyses. *Int. J. Climatol., 19,* 1375–1388, doi: 10.1002/1097-0088.

Wang, X.L., 2008a. Penalized maximal *F* test for detecting undocumented mean shift without trend change. *J. Atmos. Oceanic Tech., 25,* 368–84, doi: 10.1175/2007JTECHA982.1.

Wang, X.L. 2008b. Accounting for autocorrelation in detecting mean shifts in climate data series using the penalized maximal *t* or *F* test. *J. Appl. Meteor. Climatol., 47,* 2423–44, doi: 10.1175/2008JAMC1741.1.

Wang, X.L. and Feng, Y. 2010. RHtestsV3 User Manual. *Atmospheric Science and Technology Directorate, Science and Technology Branch, Environment Canada, Toronto*. [Available online at http://cccma.seos.uvic.ca/ETCCDMI/software.shtml].

Wang, X.L., Wen, Q.H. and Wu, Y. 2007. Penalized maximal *t* test for detecting undocumented mean change in climate data series. *J. Appl. Meteor. Climatol., 46,* 916–31, doi: 10.1175/JAM2504.1.

Wang, X.L., Chen, H., Wu, Y., Feng, Y. and Pu, Q. 2010. New techniques for the detection and adjustment of shifts in daily precipitation data series. *J. Appl. Meteor. Climatol., 49,* 2416–36, doi: 10.1175/2010JAMC2376.1.

Wen, Q.H., Wang, X.L. and Wong, A. 2011. A hybrid-domain approach for modelling climate data time series. *J. Geophys. Res. Atmos., 116,* D18112, doi: 10.1029/2011JD015850.

World Meteorological Organization. 2003. WCDMP 53—Guidelines on Climate Metadata and Homogenization. WMO–TD No. 1186, P. Llanso. Ed., 50 pp.

World Meteorological Organization. 2008. Guide to meteorological instruments and methods of observation. WMO–No. 8., 7th ed. World Meteorological Organization, Geneva.